Gasification of HYDRANE Char in Reactions with Carbon Dioxide and Steam

Walter Fuchs and Paul M. Yavorsky

U.S. Energy Research and Development Administration
Pittsburgh Energy Research Center
4800 Forbes Avenue
Pittsburgh, Pennsylvania 15213

INTRODUCTION

During the current efforts, two basic principles for coal gasification have been advanced. One is the production of synthesis gas by reacting the coal with steam under the addition of heat. If this gas should be upgraded to replace natural gas, a methanation step is necessary after the proper ratio of carbon dioxide and hydrogen has been established by a water gas shift reaction. The methanation is highly exothermic. But since it has to be executed at a moderate temperature (400° C), its heat cannot be used (1). The other possibility is to hydrogenate the coal directly under high pressure to obtain methane. This method is more efficient because it eliminates the methanation step. In the real case, direct hydrogasification does not eliminate the methanation completely, because the presence of some hydrogen in the product gas (15 to 20 pct) cannot be avoided; however, the methanation requirements are considerably less.

The HYDRANE process (2) uses the hydrogenation approach and is designed to gasify caking coal without pretreatment by partial oxidation. The caking property of the coal will be removed by feeding the raw coal into a dilute-phase reactor, in which the coal falls freely in contact with a hot gas mixture of hydrogen and methane. If the coal is heated rapidly through the plastic stage (400° C to 700° C) excessive agglomeration of the coal particles can be avoided. After the coal has been devolatilized and partly hydrogasified in the dilute phase reactor, it enters a second stage, which is a fluid bed reactor. In this stage, the solids will be hydrogasified in a hydrogen atmosphere at approximately 900° C and under a pressure of 70 atm. The gas fed to the fluid bed reactor is pure hydrogen; the gas leaving this stage contains approximately 46 pct methane. This mixture is fed to the free fall stage, where the hydrogen-to-methane conversion will continue in presence of the dilute solids phase.

Though the total carbon content of the coal could be gasified in the fluidized bed stage, it is more efficient to hydrogenate the coal only partially, and to use the remaining char for the production of the necessary hydrogen. In this case, the char leaving the fluid bed will be fed into a gasifier, in which, by adding steam and oxygen, the char will be converted into hydrogen rich synthesis gas.

Tests have been made on HYDRANE char to obtain kinetic information concerning the water gas reaction (reaction with steam). By HYDRANE char we mean the residual char rejected from the fluid bed stage of the process development unit at the ERDA Energy Research Center in Pittsburgh. This char contains approximately 50 pct of the initial carbon content of the raw coal.

Principal Reactions and Kinetics

The overall chemical reaction to be studied is

$$H_2O + \text{Char} \longrightarrow H_2 + CO + CO_2 + \text{Ash} \qquad 1)$$

This is a multistep reaction which , according to (3) and (4) among others, can be

separated into the following principal processes (C_f denotes a free reaction site and C_o an oxidized reaction site at the carbon surface):

$$H_2O + C_f \underset{k_2'}{\overset{k_2}{\rightleftharpoons}} H_2 + C_o \qquad 2)$$

$$C_o \xrightarrow{k_3} CO + \gamma C_f \qquad 3)$$

In addition, there is a competing oxygen exchange reaction

$$CO_2 + C_f \underset{k_1'}{\overset{k_1}{\rightleftharpoons}} CO + C_o \qquad 4)$$

The parameter γ in reaction (3) is assumed to be unity. In this case a steady gasification rate will be maintained; a new active site is generated with each carbon atom gasified. The experimental results tend to confirm this assumption. The number of carbon sites available for oxidation depends on the detailed structure of the surface, in addition to the surface area (5, 6, 7, 8, 9). Since the char we are dealing with is very porous, we can assume that the geometrical surface area of the particles can be neglected compared to the internal surface area, i.e., the available surface area is proportional to the total amount of solids in the reactor and independent of the size and shape of the particles.

Denote the fraction of the carbon atoms which can be oxidized (i.e., active sites) by

$$C_t = \frac{\text{Number of active sites}}{\text{Total number of carbon atoms}}$$

which is assumed to be a constant. Then the fraction of the active free sites, C_f, and of the oxidized sites, C_o, follow the relation

$$C_t = C_f + C_o \qquad 5)$$

Reaction (3) represents the actual gasification step. The gasification rate dn/dt, in mol/s is

$$-\frac{dn}{dt} = N_c = k_3 C_o n \qquad 6)$$

n is the number of carbon atoms present.

The rate constant k_3 has the dimension:

$$\frac{\text{moles gasified/second}}{\text{moles of carbon present}}$$

From Equation 6 it is easy to determine the quantity k_3C_o:

$$k_3C_o = (1/t)\ \ln\ (n_o/n(t)\ ), \qquad 7)$$

where t is the residence time of the char, and n(t) is the remaining amount of carbon in the reactor after time t. The fractional concentration of oxidized sites, C_o, is not known. It depends on the rates of the oxygen exchange reactions.

For experimental purposes we can simplify the system of reactions described above by reacting char with carbon dioxide without the presence of steam. The gasification reactivity, k_3C_o, can be determined by measuring the amount of solids converted to gas. In addition, the equilibrium value of C_o approaches very closely that of C_t if the amount of carbon monoxide generated is small compared to the carbon dioxide present; in this case almost all active sites are oxidized. This can be verified theoretically by analyzing reactions (3) and (4).

$$\frac{dC_o}{dt} = k_1 C_{CO_2} C_f - k_1' C_{CO} C_o - k_3 C_o \qquad 8)$$

C_{CO_2} and C_{CO} are the concentrations of CO_2 and CO respectively. At the high pressures of interest, the oxygen exchange reactions are very fast compared to the gasification reaction (10). Therefore, the last term of Equation 7 can be dropped. In the steady state $dC_o/dt = 0$. Eliminating the number of free sites and expressing it in terms of the total number of active sites $C_f = C_t - C_o$, we obtain

$$C_o = \frac{C_t}{1 + \frac{x}{K_1}} \qquad 9)$$

where $K_1 = k_1/k_1'$, and $x = C_{CO}/C_{CO_2}$.

Experimental Outline

The experimental system used in this study is basically the same which has been used by S. Friedman et al. (11) (see figure 1). In our application a constant flow of feed gas was maintained, which kept the char in a fluidized state. The pressure (up to 70 atm) was maintained by the supply cylinders, and in case of water, by pressurizing the water reservoir with helium. The gas flow was controlled with needle valves and flowmeters before the gas entered the reactor. A preheater was necessary to maintain a uniform temperature profile along the reactor. The reactor was heated by direct resistance heating, in which the reactor vessel served as the heating element. The heating current of up to 700A was supplied with a stepdown transformer, whose primary voltage could be controlled. The gas leaving the reactor flowed through a steam trap before it was depressurized. A back pressure regulator kept the pressure in the system constant. The gas was metered and flared. Provisions were made to take periodical gas samples for chemical analysis.

The reactor (figure 2) consisted of a 1.78 m long stainless steel tubing with an inner diameter of 0.8 cm (5/16") and a wall thickness of 0.4 cm. Two disks of porous stainless steel confined the char sample within the reaction zone, which was 1 m long. In the non-fluidized state a charge of 5 g occupies half of the reaction zone. The porous disks were kept in place by pinching the tube from the outside. A new tube had to be provided for each experiment. The temperature was monitored with four chromel-alumel thermocouples peened into the tube wall. At the bottom of the stainless steel tube, a preheater in form of a ceramic rod containing a heating wire raised the feed gas temperature.

For the steam experiments, this preheater was not sufficient to vaporize the water completely. Therefore, in addition to the preheater, heating tapes were wrapped around the water feed line to keep the temperature above the boiling point of the water at the pressure of the experiment. Extra thermocouples at the inlet and exit of the reactor allowed the temperatures to be checked to assure that no condensation has occurred.

Experimental Procedures

All experiments have been carried out isothermally at constant pressure. For the experiments with carbon dioxide and char, the reactor has been heated up rapidly after the proper gas flow has been established. The heat-up time was always less than a minute, with the run lasting between 20 minutes and 4 hours. At the conclusion of the experiment, the heat was turned off, and the reactor quenched with water. The procedure for the steam-char experiments was different. The system was first pressurized with helium, then heat was applied. After the proper temperature has been reached, the water flow was started. At the conclusion of the run, the water was turned off, and replaced with a flow of dry nitrogen in order to remove all of the steam. The reactor was slowly cooled and eventually gradually depressurized. This was necessary to avoid the condensation of water in the reactor. After the reactor has been cooled to room temperature, the stainless steel rod was cut in the middle to retrieve the residual solids, which were weighed and analyzed for their carbon contents.

Care has been taken to prevent a build up of the product gas concentration near the particle surface. This would unduly favor the back reaction of the oxygen exchange reactions. Tests showed that the superficial gas velocity to avoid this effect had to be larger than 40 cm/s for the carbon dioxide experiments, while for the steam experiments, a velocity of 15 cm/s was sufficient. This probably can be explained with the high diffusivity of hydrogen, which is the principal product of the steam - char reaction. The binary gas diffusivity of the H_2O - H_2 system is approximately 6 times that of the CO_2 - CO system (12).

Results

An analysis of the char used for most of the experiments is given in Table 1. This represents the averaged data and their standard deviation errors from eight individual analyses. The batch of char HY-13, from which these samples were taken, was always carefully mixed before a sample was withdrawn. As can be seen, the only major components are carbon and ash. In a few cases char from a different source has been used; this is discussed below.

Carbon dioxide - char reactions:

Since the carbon dioxide - char reaction experiments are less complicated and easier to analyze than the steam - char reactions, they have been carried out first. All pertinent data are listed in Table 2. The temperature ranged from 750° C to 900° C. The pressure was usually 35 atm, and twice it was 18 atm. The feed gas was a mixture of carbon dioxide and helium. In most cases the ratio was 1 part helium to 10 parts carbon dioxide. The partial pressure of the carbon dioxide is given in column 3. The feed was adjusted such that the linear gas velocity for most tests was kept between 0.4 and 0.6 m/s (column 4), requiring a gas flow of up to 0.010 mol/s; this is a very high gas feed compared to the actual conversions, such that more than 99 pct of the effluent gas consists of carbon dioxide and helium. The carbon monoxide production was almost not measurable (<0.5%). However, the solids and carbon conversion was determined. Column 6 gives the fraction of the retrieved solids by weight (i.e., X = weight of residual solids/weight of charge). The fraction of the retrieved carbon has been determined by chemical analysis of the charge and of the residue and is listed in column 7 (i.e., Y = mass of carbon in the residuum/mass of carbon in the charge). In figure 3 the quantity Y is plotted versus X. The graph also contains points obtained from steam experiments. All points are scattered around a straight line intersecting the abscissa at 0.32, which corresponds to the ash content of the original char (see Table 1). One can conclude that, while the ash remains completely inert, the

non-ash components, which consist to 97 pct of carbon, are gasified at the same rate as the fixed carbon. This observation allows to calculate the carbon conversion from the total mass loss, which is determined by weighing and therefore many times more accurate than a chemical analysis of the residual solids. The fractional carbon conversion (equivalent to the quantity Y in Table 2) can be expressed as

$$Y = \frac{X - C_A}{1 - C_A}, \qquad 10)$$

where C_A is the fractional ash content of the charge. The reaction constant in column 8 of Table 2 is calculated according to Equations 7 and 10

$$B = \frac{1}{t_{res}} \ln \frac{1 - C_A}{X - C_A} \qquad 11)$$

where t_{res} is the residence time given in column 5 of Table 2. The results show that the carbon conversion is a first order process with regard to the carbon present. Figure 4 shows no systematic relationship between the rate constant as defined in Equation 7 and the mass loss. The Arrhenius plot in figure 5 shows that the process is also of 0th order with regard to the amount of reactant gas present. Two data points have been obtained from experiments conducted at 18 atm, which is half the usual pressure (see Table 2). The Arrhenius plot yields an activation energy of 54.5 kcal/mol and a frequency factor of $1.14 \times 10^7 s^{-1}$. The plotted quantities represent the rate constant k_3C_o as it is defined in Equation 6. However, as already mentioned, with the low carbon monoxide concentration ($\leq 0.5\%$), the quantity C_o is approaching C_t according to Equation 9. K_1 is the equilibrium constant for the oxygen exchange reactions 4, and assumes the values from 0.03 to 0.2 for a temperature range between 750° C and 900° C (4, 13). Using these figures and Equation 10, it has been estimated that the quantity k_3C_t should be in the average 10 pct larger than B, with an activation energy reduced by approximately 2 kcal/mol. But this is within the fluctuation of the experimental data. Table 2 and figure 5 contain 3 points taken on SYNTHANE char at three different temperatures. This material, originally Illinois #6 coal, went through a steam gasification process with 60 pct of its original carbon content gasified. The reactivity of this char cannot be distinguished from the HYDRANE char.

Steam - Char Reaction:

The reaction of the char with steam is a more involved process than the carbon dioxide reaction because now reactions 2 and 4 compete with each other. Also with the existing experimental system, the temperature along the reactor could not be kept as uniform as was the case with the carbon dioxide experiments, causing more scattering of the data. Results of the steam series are listed in Table 3. The arrangement of the columns is the same as in Table 2, except no partial pressure is given because the feed gas consisted exclusively of steam. Since the carbon conversion data from these runs have the same relationship to the total mass loss as was the case with the carbon dioxide experiments, Equation 11 could also be used to calculate the rate constant. An Arrhenius plot of the rate constants is given in figure 6 superimposed on the averaged rate constant for the carbon dioxide - char reaction taken from figure 5. Taking the experimental scattering into account, we see that for both types of reactions the reactivity is similar. Since the steam concentration was always more than 98 pct, the difference between C_o and C_t can be assumed to be

very small, using the same argument as for the carbon dioxide tests. The similarity between the carbon dioxide and the steam data indicate that the gasification reaction, Equation 3, is the rate controlling step, with the same type of reaction sites responsible for both reactions. Also it has been shown that the concentration of the reactant gas has no effect on the reactivity.

Discussion

The reactivities obtained in our experiments refer to the composite quantity k_3C_t, where C_t is assumed to be independent of the temperature (within the limits of our experimental conditions). C_t represents the fraction of those carbon atoms in the solid which are available for oxidation. Obviously, the surface area of the material is of prime importance. However, as already mentioned, only a small portion of the surface sites is capable of accepting oxygen. In graphites, this portion is 4 pct (9). Moreover, it was shown that various discrete types of reactive sites do exist on graphon surfaces (5, 6, 7, 8), which in general are activated at different temperature regimes. The accepted notion is that oxidation takes place around crystallographic defects (14). Following these arguments, it should be expected that the gasification reactivities of chars and cokes, with their high surface area and their high structural disorder, should be many times larger than those of graphitized materials. In figure 7 the reactivity constants for gasification, k_3C_t, of various graphites and carbons, obtained by Ergun (4) and Mentser and Ergun (10) are plotted together with our results from the carbon dioxide - char reaction experiments.

The activation energy remains the same for all materials. In addition, the activation energy from recent experiments on reactions of petroleum coke and electrode material with carbon dioxide (17) is between 51.3 and 56.6 kcal/mol, in good agreement with our data. This allows the conclusion that the chemical desorption step, which according to Equation 3 is controlled by the quantity k_3, is unaffected by the crystallographic state of the reactive surface. However, the fraction of available active sites, C_t, varies by more than 2 orders of magnitude, as can be seen from the pre-exponential factors of the Arrhenius plots in figure 7. The lowest C_t is associated with Ceylon graphite, which comes closest to an ideal graphite structure. The reactivity of the materials follows inversely the order of their degree of crystallographic perfection.

The first order characteristic of the carbon conversion process is in agreement with the assumption that, for a particular material, the fraction of the active sites, C_t, remains constant during the reaction, or, in other words, that the parameter γ in the gasification reaction, Equation 3, in unity. This has been confirmed by surface area measurements, which showed that the B. E. T. surface of a sample before and after the experiment increased only slightly.

A catalytic effect due to the multitude of foreign matter in cokes and chars is possible. However, this should also change the activation energy of the gasification step. Experimental evidence suggests that the activation energy should decrease with catalytic action (15).

Experiments on various types of chars and raw coals under atmospheric pressure have been conducted by C. Y. Wen's group in Morgantown, West Virginia, (16). Figure 8 shows the results as continuous curves. An interesting feature is that the pre-exponential factor depends only on the source of the coal, and not on the treatment for charring. The upper curve describes the reaction behaviors of untreated Illinois #6 coal and three different chars made from Illinois #6 (HYDRANE, SYNTHANE, IGT) the lower curve refers to untreated Pittsburgh Seam coal and to HYDRANE char made from this coal. The bottom curve in figure 8 refers to measurements by Ergun (13) on metallurgic coke. The activation energies of all three curves agree well with the results of this study up to a temperature of approximately 1000° C. Above that

temperature, the activation energies decrease markedly. Various explanations have been suggested for this behavior.

Conclusion

For temperatures up to 1000° C and within a wide pressure range (from atmospheric to 70 atm), the rate limiting step for the reaction of carbon with steam as well as with carbon dioxide is the desorption reaction, in which an oxidized carbon is released from the carbon surface, forming a gaseous carbon monoxide molecule. This process is governed by an activation energy around 56 kcal/mol. It is suggested that for both reactions, steam - carbon and carbon dioxide - carbon, the same type of atomic carbon sites on the surface are involved. In addition, it has been shown that chars made from Illinois #6 coal exhibit high reactivities compared to other carbonaceous materials. This probably is due to a large surface area and a high crystallographic disorder of the char.

ACKNOWLEDGEMENT

Fruitful discussions with Dr. S. Ergun are greatly appreciated.

REFERENCES

1. Forney, A. J. and J. P. McGee, 4th Synthetic Pipeline Gas Symposium, Chicago, Illinois, p. 51 (1972).

2. Wen, C. Y., S. Mori, J. A. Gray, and P. M. Yavorsky, 67th Annual AIChE Meeting, Washington, D. C. (December 1974).

3. Reif, A. E., J. Phys. Chem. 56, 785 (1952).

4. Ergun, S., J. Phys. Chem. 60, 480 (1956).

5. Phillips, R., F. J. Vastola, and P. L. Walker, Jr., 3rd Conference on Industrial Carbon and Graphite, London, 1970, p. 257.

6. Bansal, R. C., F. J. Vastola, and P. L. Walker, Jr., Carbon 8, 443 (1970).

7. Phillips, R., F. J. Vastola, and P. L. Walker, Jr., Carbon 8, 197 (1970).

8. Wiesmann, U., Carbon 8, 105 (1970).

9. Walker, P. L., Jr., L. G. Austin, and J. J. Tietjen, Chemistry and Physics of Carbon, Vol. 1 (P. L. Walker, Jr., ed.) Dekker, New York, 1965, p. 328.

10. Mentser, M. and S. Ergun, Bureau of Mines Bulletin 664, Washington, D. C., 1973

11. Friedman, S., P. S. Lewis, R. D. Graves, and R. W. Hiteshue, Bureau of Mines Report of Investigation 7209, Washington, D. C. 1968.

12. Janka, J. C., and R. Malhotra, Estimation of Coal and Gas Properties for Gasification Design Calculations, Institute of Gas Technology, Chicago, Illinois, 1971.

13. Ergun, S., Bureau of Mines Bulletin 598, Washington, D. C., 1962.

14. Thomas, J. M., Chemistry and Physics of Carbon, Vol. 1 (P. L. Walker, Jr. ed.) Dekker, New York, 1965, p. 122.

15. Walker, P. L., Jr., M. Shelef, and R. A. Anderson, Chemistry and Physics of Physics of Carbon, Vol. 4 (P. L. Walker, Jr., ed.) Dekker, New York, 1968.

16. Wen, C. Y., private communication.

17. Tyler, R. J. and I. W. Smith, Fuel 54, 99 (1975).

TABLE 1.- Analysis of HYDRANE char
(HY-13, made from Illinois #6)

	As received	Moisture and ash free
Proximate Analysis		
Moisture	3.5 ± 0.4	
Volatile Matter	3.5 ± 1.5	4.2 ± 0.8
Fixed Carbon	61.1 ± 4.8	95.8 ± 0.8
Ash	31.9 ± 3.8	
Ultimate Analysis		
Hydrogen	1.1 ± 0.1	1.2 ± 0.3
Carbon	61.8 ± 3.1	96.6 ± 0.6
Nitrogen	0.4 ± 0.05	0.7 ± 0.05
Oxygen	3.6 ± 0.2	0.6 ± 0.2
Sulfur	0.6 ± 0.05	0.9 ± 0.05
Ash	32.5 ± 3.4	

TABLE 2.- Results of the CO_2-char reaction experiments

Temperature, °C	Pressure Total atm	Pressure Partial atm	Gas velocity, m/sec	Residence time, min	Retrieved solids X	Retrieved carbon Y	Rate constant 10^{-4} sec^{-1}	Material
750	35	31.8	0.49	120	0.827	0.764	0.518	
750	35	31.8	.49	120	.898		.228	
750	35	31.8	.49	120	.849	.825	.352	
750	35	31.8	.49	240	.728	.659	.239	
750	35	31.8	.49	360	.671	.461	.309	
750	18	16.4	.49	120	.872	.818	.292	
790	35	17.5	.60	120	.748	.668	.649	
795	35	26.25	.60	120	.759	.538	.613	HYDRANE
800	35	31.8	.50	120	.626	.442	1.122	char
800	35	31.8	.50	60	.818	.656	0.873	
800	35	31.8	.50	240	.489	.225	.982	
800	35	31.8	.50	180	.555	.406	.997	
800	18	16.4	.49	120	.722	.589	.843	
850	35	31.8	.54	60	.534	.341	3.257	
850	35	31.8	.54	90	.442	.174	3.245	
850	35	31.8	.54	30	.677	.557	3.617	
900	35	26.25	.66	20	.553		9.04	
750	35	31.8	0.49	240	0.779	0.723	0.311	SYNTHANE
800	35	31.8	.50	60	.786	.766	1.196	char
850	35	31.8	.54	45	.606	.394	3.829	

TABLE 3.- Results of the steam-char reaction experiments

Temperature, °C	Total pressure, atm	Gas velocity, m/sec	Residence time, min	Retrieved solids X	Retrieved carbon Y	Rate constant, 10^{-4} sec^{-1}
700	35	0.13	120	0.8908	0.7732	0.246
800	35	0.15	120	.612	.412	1.193
800	35	0.10	120	.640	.462	1.062
800	69	0.077	120	.565	.366	1.443
800	18	0.28	120	.526	.306	1.691
830	35	0.15	120	.454	.311	2.313
900	35	0.16	60	.366	.0583	7.892
900	35	0.16	180	.356	.0640	2.906

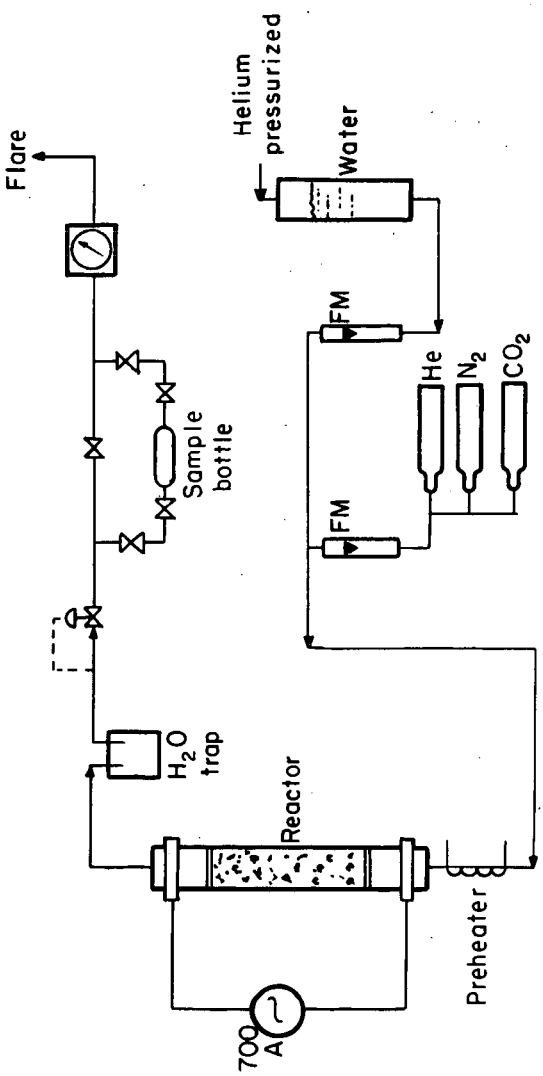

Figure 1— Reaction kinetics experiment simplified flow diagram.

L-14324

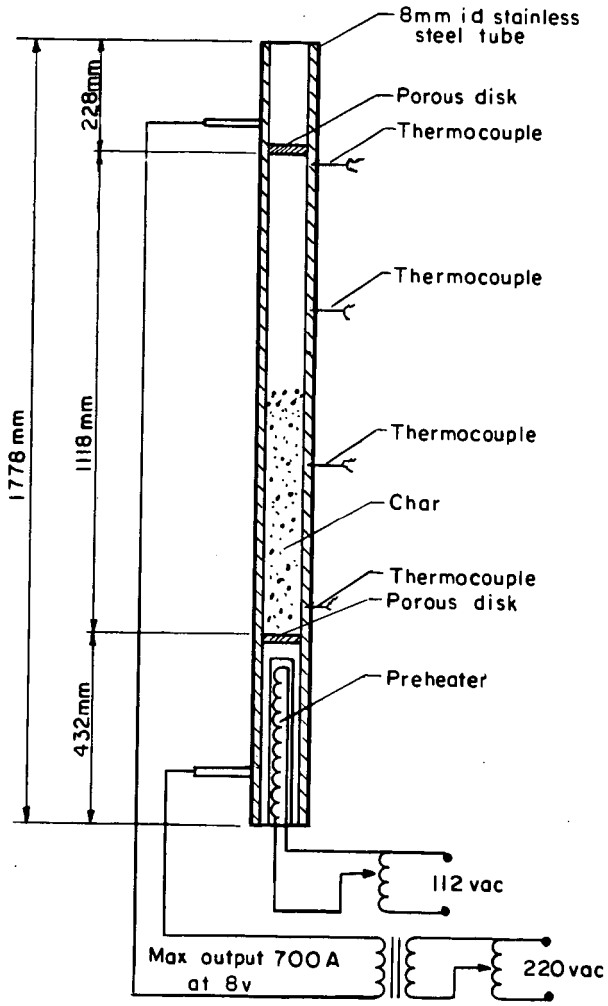

Figure 2—Details of reactor.

L-14325

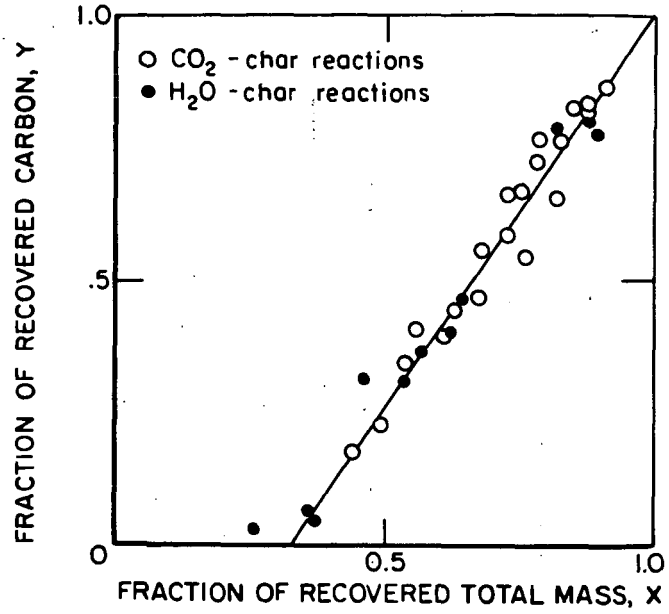

Figure 3—Relationship between the converted carbon and the mass loss

L-14326

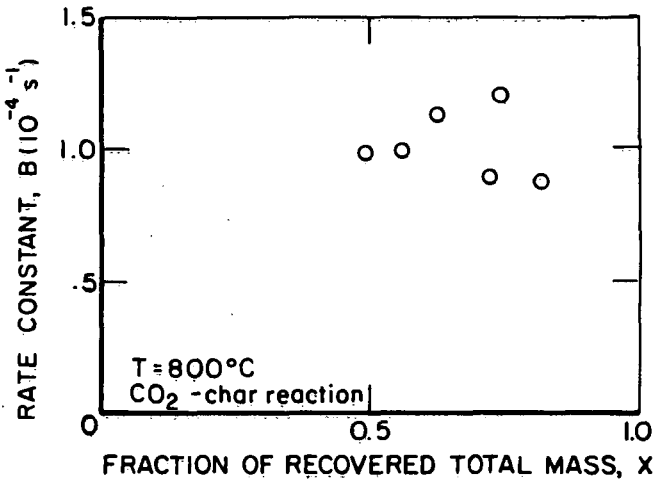

Figure 4—Test for 1st order reaction of the carbon conversion.

L-14327

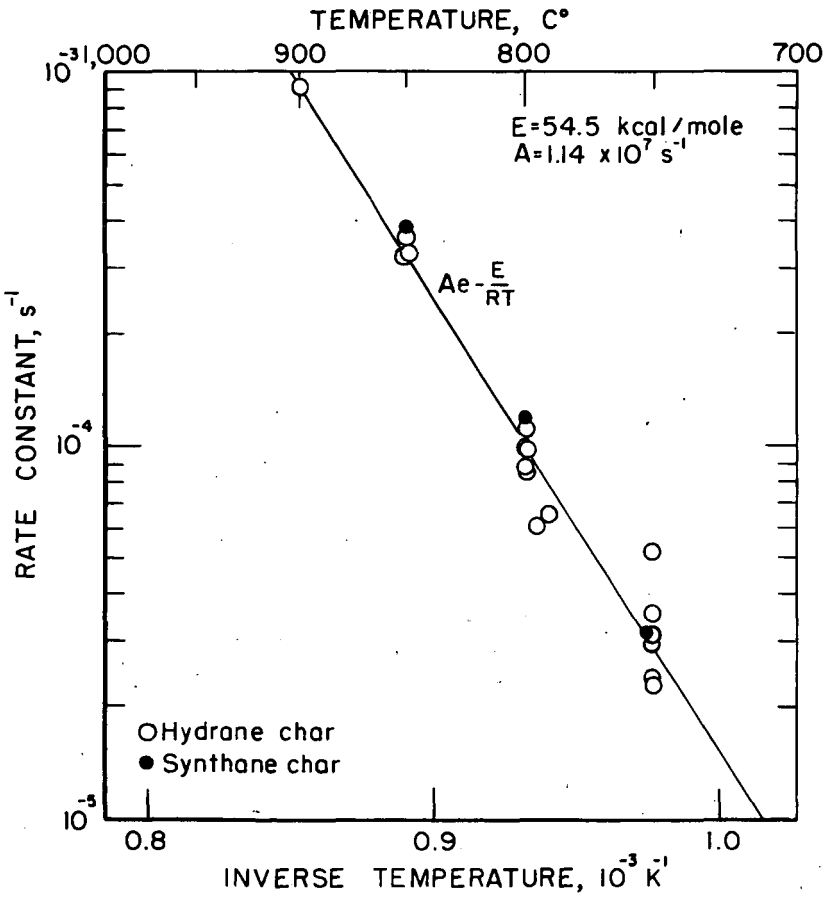

Figure 5—Gasification rate constant for the reaction of CO_2 with char.

L-14328

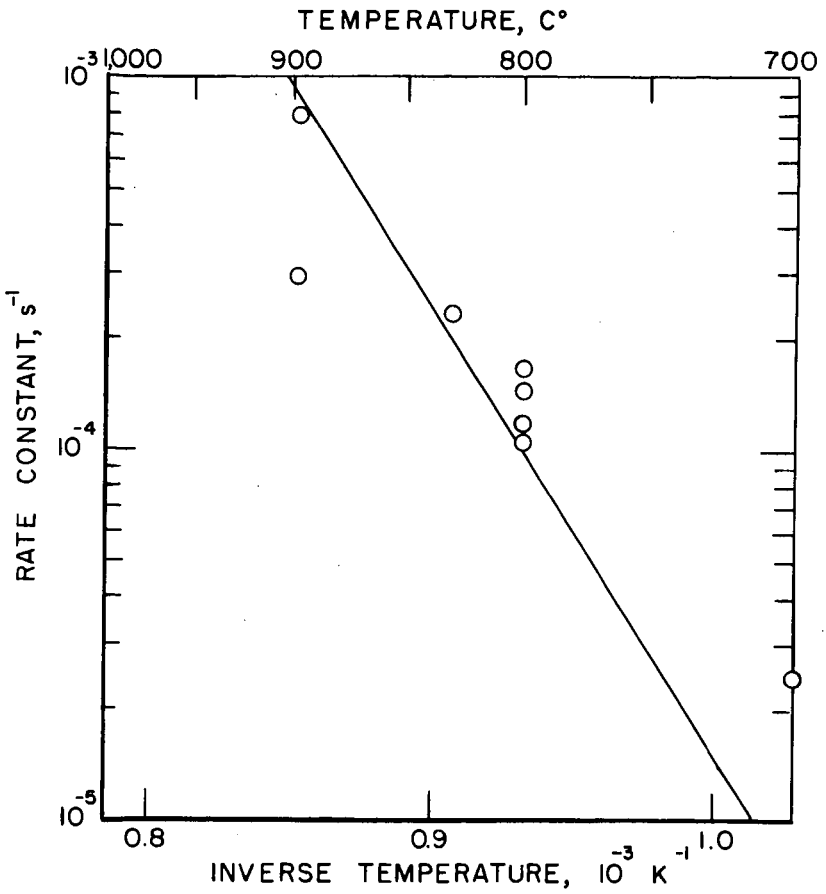

Figure 6—Gasification rate constant for the reaction of steam with hydrane char (The continuous line represents the rate constant for the CO_2 char reaction)

L-14329

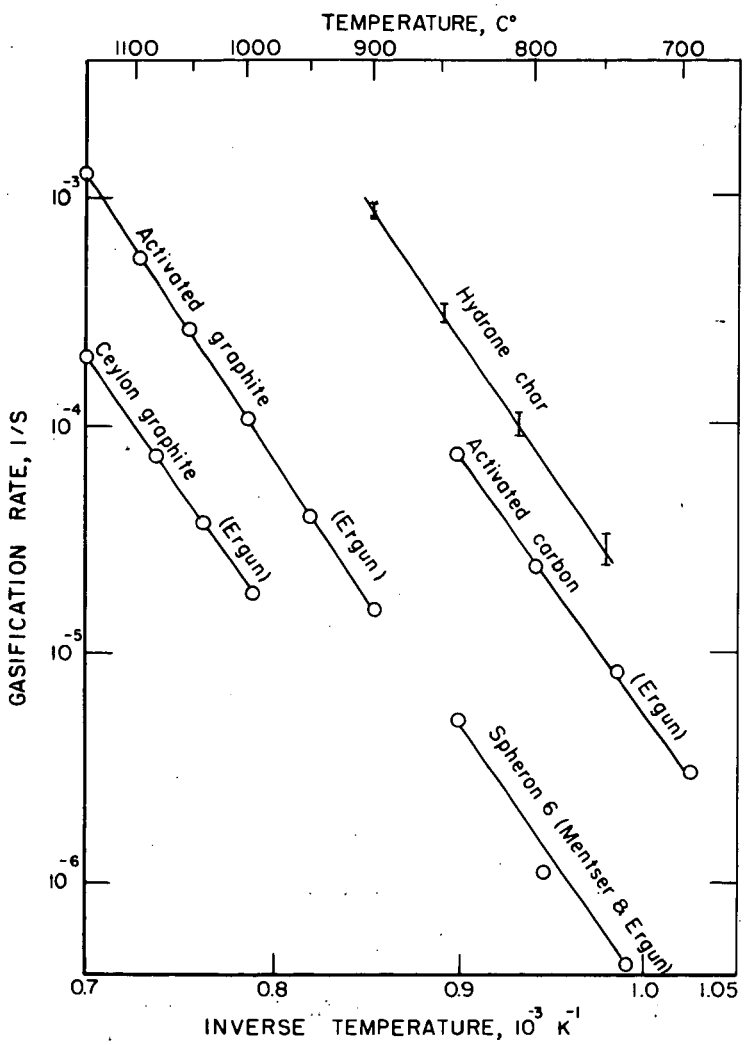

Figure 7 — Temperature variation of gasification rate constants of graphite and carbons.

L-14330

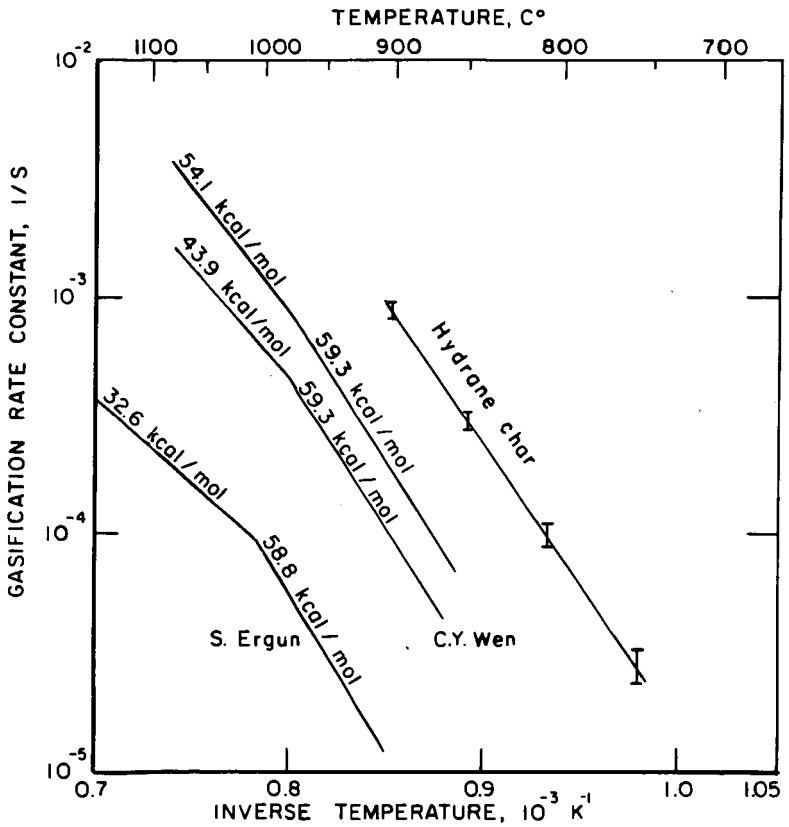

Figure 8—Temperature variation of gasification rate constants of cokes and chars.

L-14331